

Discovery and SAR of Natural-Product-Inspired RXR Agonists with Heterodimer Selectivity to PPAR δ -RXR

Ken-ichi Nakashima,^{*, \perp} Eiji Yamaguchi, ^{\perp} Chihaya Noritake, Yukari Mitsugi, Mayuki Goto, Takao Hirai, Naohito Abe, Eiji Sakai, Masayoshi Oyama, Akichika Itoh, and Makoto Inoue



Cite This: <https://dx.doi.org/10.1021/acscchembio.0c00146>



Read Online

ACCESS |



Metrics & More

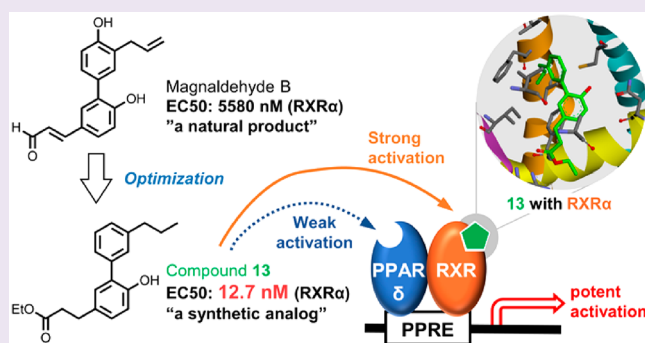


Article Recommendations



Supporting Information

ABSTRACT: A known natural product, magnaldehyde B, was identified as an agonist of retinoid X receptor (RXR) α . Magnaldehyde B was isolated from *Magnolia obovata* (Magnoliaceae) and synthesized along with more potent analogs for screening of their RXR α agonistic activities. Structural optimization of magnaldehyde B resulted in the development of a candidate molecule that displayed a 440-fold increase in potency. Receptor–ligand docking simulations indicated that this molecule has the highest affinity with the ligand binding domain of RXR α among the analogs synthesized in this study. Furthermore, the selective activation of the peroxisome proliferator-activated receptor (PPAR) δ -RXR heterodimer with a stronger efficacy compared to those of PPAR α -RXR and PPAR γ -RXR was achieved in luciferase reporter assays using the PPAR response element driven reporter (PPRE-Luc). The PPAR δ activity of the molecule was significantly inhibited by the antagonists of both RXR and PPAR δ , whereas the activity of GW501516 was not affected by the RXR antagonist. Furthermore, the molecule exhibited a particularly weak PPAR δ agonistic activity in reporter gene assays using the Gal4 hybrid system. The obtained data therefore suggest that the weak PPAR δ agonistic activity of the optimized molecule is synergistically enhanced by its own RXR agonistic activity, indicating the potent agonistic activity of the PPAR δ -RXR heterodimer.



INTRODUCTION

The retinoid X receptor (RXR) is an important member of the ligand-dependent nuclear receptor (NR) family. RXR is a unique and ubiquitous heterodimeric partner for the NR signaling pathway, and it forms homodimers or heterodimers with retinoic acid receptors (RAR), peroxisome proliferator-activated receptors (PPARs), liver X receptors (LXRs), thyroid hormone receptors (TRs), vitamin D receptors (VDRs), nuclear receptor related-1 protein (Nurr1), and related receptors.^{1,2} The NR-RXR heterodimers and the RXR homodimer bind to specific response elements on DNA and regulate the transactivation of target genes, and the molecular dynamics mechanism underlying this ligand binding-induced activation has been revealed in the structural analysis of NRs.^{3–5} In the absence of ligands, corepressor proteins bind to the surface of NRs and cause the repositioning of C-terminal helix 12, which is a key structural component of the activating function 2 (AF2) domain. The binding of agonists to the ligand binding domain (LBD), which is composed of 12 α -helices (H1–12) with two small β -sheets between H5 and H6 (β -turn), leads to a cascade of events culminating in the repositioning and stabilization of H12 and several other helices to form the AF2 surface, which possesses a binding capacity for the LXXLL motif of coactivators. NMR studies into apo-NRs⁶

revealed the absence or broadening of signals corresponding to residues within the ligand binding pocket and the AF2 surface, suggesting that these regions do not distribute in a particular conformation. In contrast, the detection or sharpening of the corresponding signals in holo-NRs suggests stabilization of the LBD in the active conformation due to ligand binding to NRs. RXR heterodimers can be classified into “permissive” and “nonpermissive” heterodimers,^{7–10} whereby the activation of permissive heterodimers, such as PPAR-RXR and RXR-LXR, is possible by the binding of RXR agonists alone. On the other hand, nonpermissive heterodimers, such as RXR-RAR, RXR-TR, and VDR-RXR, are silenced by the binding of RXR agonists only. Analysis of the structural and dynamic differences between PPAR γ -RXR α , a “permissive” heterodimer, and RXR α -TR β , a “non-permissive” heterodimer using NMR spectroscopy, X-ray crystallography, and hydrogen/deuterium exchange mass spectrometry (MS), revealed that

Received: February 28, 2020

Accepted: April 23, 2020

TR β reduces the stability of holo-RXR α LBD in the active conformation by dimerization, whereas PPAR γ does not exhibit such an effect.⁶

Among the various known RXR heterodimers, the available therapeutic approaches mostly target PPAR-RXR. The three subtypes of the PPAR family, namely PPAR α , PPAR γ , and PPAR δ (also known as PPAR β/δ), differ in tissue distribution and their role in biological systems.^{11,12} More specifically, PPAR γ is the most studied subtype of the PPAR family and is expressed abundantly in adipose tissues, the large intestine, and hematopoietic cells, and plays a critical role in the regulation of adipogenesis, insulin sensitivity, and lipid metabolism.^{12,13} Thiazolidinediones (e.g., rosiglitazone and pioglitazone) are the only class of clinically used PPAR γ agonist therapeutics for the treatment of type 2 diabetes mellitus to ameliorate insulin resistance.^{14,15} PPAR α is expressed abundantly in the liver, colon crypt, and myocardium.¹² Fibrates (e.g., bezafibrate and fenofibrate) are PPAR α agonists used clinically for the treatment of hypercholesterolemia and hypertriglyceridemia. Although proven therapies targeting PPAR γ and PPAR α are known, prescription drugs for targeting PPAR δ , which is ubiquitously expressed in most tissues and is known to regulate lipid metabolism and glucose homeostasis,¹² do not exist due to the serious side effects observed with the use of known agonists.^{16,17} However, research aimed at addressing these challenges is ongoing, and preclinical studies using certain synthetic PPAR δ agonists (e.g., GW501516 and GW0742) have found benefits against obesity-induced insulin resistance, type 2 diabetes mellitus, and cardiovascular disease.^{18–20} In this context, the development of new PPAR δ agonists to reduce these adverse effects and conditions is highly important and will be useful for treating type 2 diabetes mellitus, and as such, is the objective of this study. Regardless of their effects in permissive or nonpermissive heterodimers, RXR agonists concertedly enhance transactivation as partner NR agonists.^{7,21} Although the functional elucidation of RXR has not been completely achieved due to multiple signaling pathways involving RXR heterodimers, RXR is considered an attractive target for drug discovery.²² Indeed, bexarotene (targretin), a selective RXR ligand, has been clinically used for the treatment of cutaneous T cell lymphoma. In addition, 9-*cis* retinoic acid, a ligand for both RXR and RAR, has been used in the treatment of Kaposi's sarcoma and chronic hand eczema. Furthermore, various studies have indicated the beneficial effects of RXR agonists against type 2 diabetes mellitus^{23,24} and Alzheimer's disease,²⁵ although their efficiency for the treatment of Alzheimer's disease has been controversial.

We have been interested in the discovery and evaluation of RXR ligands from natural resources and have previously reported studies that honokiol isolated from the bark of *Magnolia obovata* (Magnoliaceae) is an RXR agonist.²⁶ Honokiol activates RXR α at a half-maximal effective concentration (EC₅₀) of 16.5 μ M in the luciferase reporter assay (Figure 1). However, this compound showed a much lower potency than that of bexarotene (EC₅₀: 18.7 nM). In addition, honokiol exhibited a maximum activation of only 28.6% relative to the 100 nM concentration of bexarotene. In our quest to find agonists of higher potency and efficacy, we carried out further chemical investigations of the roots of *M. obovata* in an unpublished preliminary study. Indeed, we identified a known neolignan magnaldehyde B (**1**)²⁷ to be a more effective against RXR α than honokiol. Magnaldehyde B (**1**) activated RXR α with an EC₅₀ value of 5.58 μ M and

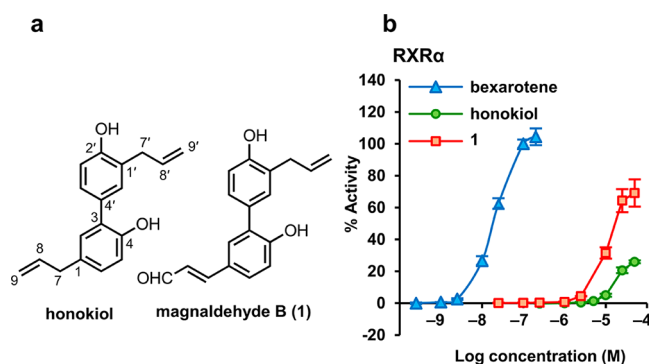


Figure 1. Magnaldehyde B (**1**) is a more effective RXR α agonist than honokiol. (a) Structures of honokiol and **1**. (b) RXR α agonistic activities of honokiol and **1** with bexarotene. Data are means \pm SD (SD = standard deviation) of three biological replicates.

displayed an E_{\max} of 79.4% in the luciferase reporter assay (Figure 1). Furthermore, we previously carried out receptor–ligand docking simulations, which indicated that the carbonyl group within drupanin (i.e., 3-phenyl-4-hydroxy-*trans*-cinnamic acid) plays a vital role in the formation of hydrogen bonds with Arg316,²⁸ which is a key residue for activation of the receptor.^{29,30} Magnaldehyde B (**1**) also contains a phenylpropanoid unit with an aldehyde group which points to the importance of the aldehyde carbonyl functionality as an essential structural element for the activation of RXR.

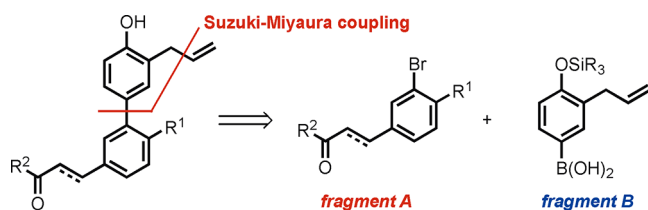
Recently, Scheepstra et al. reported that honokiol targets both sides of the AF-2 domain in RXR, and they analyzed the dual-binding behavior of honokiol in a twofold approach with a ligand binding pocket side and a coactivator binding side being the two binding modes.³¹ The same research group also discovered potent agonists for the RXR homodimer and the RXR-Nurr1 heterodimer.³² Although the activity and mode of action of honokiol are known to a certain extent, no structure–activity relationship (SAR) studies on the RXR agonistic activity of honokiol derivatives have been reported prior to this work, and so we sought to evaluate RXR agonistic activities of **1** and its analogs to improve their activities and render them potential candidates for therapeutic development. Furthermore, we investigate the ability of the synthesized agonists to activate the PPAR δ -RXR heterodimer selectively over PPAR α - and PPAR γ -RXR heterodimers by a nonconventional mechanism.

RESULTS AND DISCUSSION

Structural Optimization of Magnaldehyde B. We envisioned the retrosynthesis of the biaryl targets via the key disconnection to the aryl bromide fragment A and the arylboronic acid fragment B, which could be coupled together in the forward synthesis employing a Suzuki–Miyaura coupling protocol in a unified divergent approach to **1** and its analogs (Scheme 1). The synthetic pathway for the preparation of **1–8** is shown in Scheme 2.

We began the synthesis of the magnaldehyde B analogs with the preparation of a range of substituted fragment A derivatives. The Horner–Wadsworth–Emmons reaction of the TBS-protected aldehyde **19** afforded the desired fragment A (**20**) in good yield. A subsequent DIBAL-mediated 1,2-reduction of **20** followed by MnO₂ oxidation of the resultant alcohol afforded **21**. The 1,4-reduction of **20a** using CoCl₂ and NaBH₄ furnished the reduced derivative **22a** in 89% yield.

Scheme 1. Retrosynthetic Analysis for Magnaldehyde B Analogs



Hydrogenation of **20b** under a hydrogen atmosphere with Pd/C catalysis delivered **22b** in a quantitative yield. The corresponding aldehyde **23** was synthesized by the LiAlH₄ reduction of **22**, followed by a Dess–Martin oxidation of the obtained alcohol. However, acetal protection of the formed aldehyde **23b** was required due to its instability.

The synthesis of fragment B began with the allylation of 4-bromophenol **25**, followed by a Claisen rearrangement and TBS protection of the resultant phenol. The transformation of **26** through a halogen-metal exchange/borylation sequence furnished the desired fragment B (**27**) in an excellent yield (88% overall yield). With the two fragments in hand, a Suzuki–Miyaura coupling was performed. The reaction of aryl bromides **20–24** with boronic acid **27** using the Pd₂(dba)₃ and X-Phos system in the presence of K₂CO₃ as the base in a mixture of THF/H₂O at 95 °C, followed by deprotection of the coupled products afforded the corresponding biaryl products **1–8** in moderate to good yields.

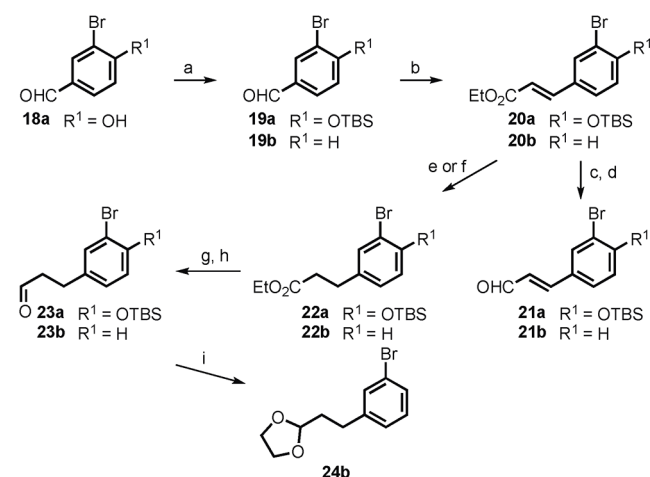
The RXR α agonistic activities of **1–8** are included in Table 1, whereby it is apparent that molecules bearing a hydroxy group at the C-4 position (**1**, **3**, **5**, and **7**) displayed significantly lower EC₅₀ values than those of their analogs without this group (**2**, **4**, **6**, and **8**, respectively). Furthermore, the obtained results indicate that the presence of a double bond between the C-8' and C-9' atoms was likely to negatively impact the agonistic activity. In compounds **1–8**, compound **7** exhibited the highest potency (EC₅₀ = 260 nM) for the activation of RXR α . Following our achievement of the optimal substitutions for fragment A, we decided to further modify fragment B of **7**. In addition, we modified fragment A of **8** to confirm the necessity for the presence of a hydroxy group at the C-4 position.

As shown in Scheme 3, various modified fragment B boronic acids were synthesized and employed in the Suzuki–Miyaura cross-coupling reactions. The hydrogenation of **27** using Pd/C proceeded quantitatively to afford the propyl substituted boronic acid **28**. Borylation of 3-allyl bromobenzene **29** was performed to furnish corresponding des-hydroxy fragment B, **30**, and subsequent hydrogenation of **30** delivered 3-propyl benzenboronic acid **31** in a quantitative yield. With all desired fragments in hand, the Suzuki–Miyaura coupling of fragments A and B was performed employing the previously developed coupling conditions, giving the corresponding coupled products **9–14** in good yields.

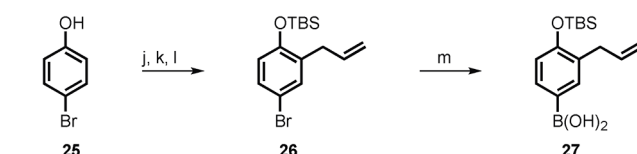
The RXR α agonistic activities of the synthesized series **9–14** were also examined, and the results are presented in Table 1. Similar to their analogs **1–8**, compounds bearing a hydroxy group at the C-4 position (**9**, **11**, and **13**) displayed significantly lower EC₅₀ values than those of their nonhydroxy analogs (**10**, **12**, and **14**, respectively). On the other hand, molecules with a hydroxy group at the C-2' position (**7**, **8**, **11**, and **12**) gave higher EC₅₀ values than those of their

Scheme 2. Synthesis of **1–8**^a

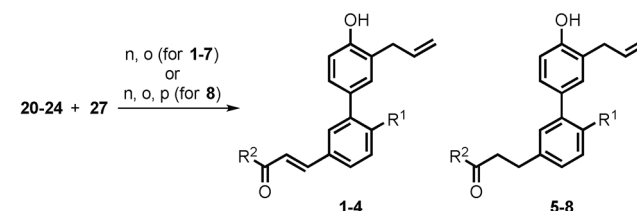
● Synthesis of fragment A



● Synthesis of fragment B



● Suzuki–Miyaura cross-coupling reaction



	R ¹	R ²	yield (%)
1	OH	H	36
2	H	H	52
3	OH	OEt	49
4	H	OEt	72
5	OH	H	63
6	H	H	28
7	OH	OEt	78
8	H	OEt	69

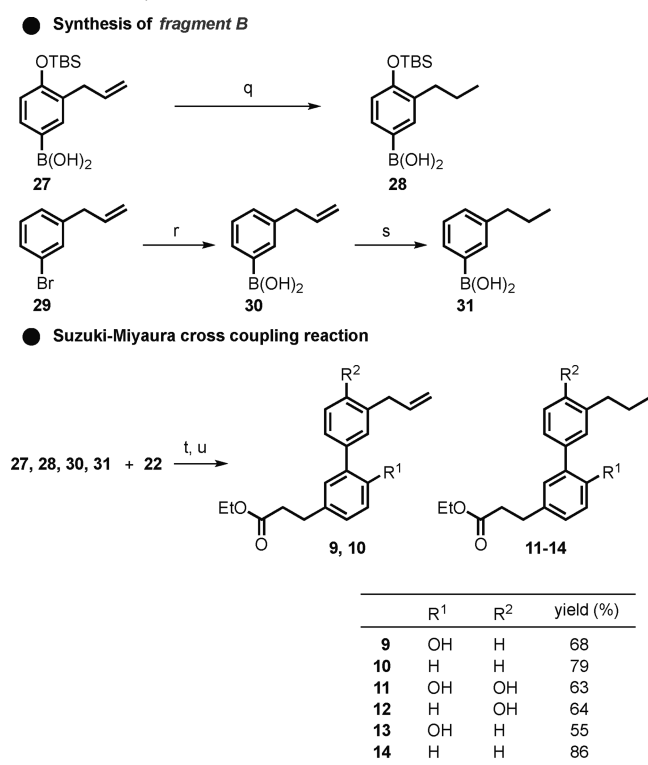
^aReagents and conditions: (a) TBSCl, imidazole, DCM, 0 °C, then rt, 16 h, 98%; (b) NaH, ethyl 2-phosphonoacetate, THF, 0 °C then rt, 1 h, **20a** 90%, **20b** 85%; (c) DIBAL-H, THF, −78 °C; (d) MnO₂, DCM, rt, 2 days. **21a** 48% (2 steps), **21b** 98% (2 steps); (e) NaBH₄, CoCl₂, MeOH, −10 °C, 30 min, **22a** 89%; (f) Pd/C, H₂, EtOH, rt, 16 h, **22b** quant.; (g) LAH, THF, 0 °C, 1 h; (h) DMP, DCM, rt, 3 h, **23a** 72% (2 steps); (i) ethylene glycol, PTSA, toluene, reflux, 16 h, **23b** 58% (3 steps); (j) allyl bromide, K₂CO₃, DMF, 60 °C, 1 h, 99%; (k) 200 °C, 3 h, 92%; (l) TBSCl, imidazole, DMF, rt, 16 h, 97%; (m) *n*-BuLi, THF, −78 °C 1 h then B(Oi-Pr)₃, −78 °C to rt, 16 h, 90%; (n) Pd₂(dba)₃, X-Phos, K₂CO₃, THF, H₂O, 95 °C; (o) TBFAF, THF, 0 °C then rt, 16 h; (p) HCl aq., 3 h.

nonhydroxy analogs (**9**, **10**, **13**, and **14**, respectively), which indicates that the absence of the hydroxy group at the C-2' position contributes to a reduction in the EC₅₀ value. Therefore, compound **13**, which possessed the best substitution pattern, displayed the greatest potency (12.7 nM) among the various test compounds evaluated herein. Furthermore, the activity of **13** was comparable to that of the full-agonist, bexarotene.

Table 1. RXR α Agonistic Activities and Calculated Docking Affinities of 1–14

compounds	EC ₅₀ (nM) ^a	E _{max} (%) ^b	calculated affinity (kcal/mol) ^c
bexarotene	18.7 ± 2.1	100	−12.9
honokiol	16 500 ± 1240	28.6 ± 8.7	−10.0
1	5580 ± 820	79.4 ± 3.9	−10.5
2	8140 ± 730	49.0 ± 3.0	−10.3
3	1310 ± 130	46.9 ± 5.4	−10.4
4	10 300 ± 100	65.0 ± 4.3	−10.5
5	824 ± 190	53.7 ± 3.2	−10.1
6	2460 ± 240	48.6 ± 5.4	−10.2
7	260 ± 10	55.7 ± 5.6	−10.6
8	10 200 ± 800	57.4 ± 11.8	−10.7
9	23.0 ± 1.7	69.8 ± 2.4	−11.1
10	4720 ± 920	85.5 ± 8.9	−10.6
11	180 ± 11	60.4 ± 3.0	−10.8
12	7070 ± 2380	67.5 ± 8.2	−10.7
13	12.7 ± 1.1	71.3 ± 9.3	−11.2
14	1810 ± 80	67.0 ± 8.4	−10.7

^aEC₅₀ values are presented as mean ± SD of three independent experiments (SD is standard deviation). ^bE_{max} data are presented as mean ± SD of the maximum activation relative to the bexarotene-induced maximum activation for RXR α . ^cCalculated affinities are best scores obtained from Autodock Vina.

Scheme 3. Synthesis of 9–14^a

^aReagents and conditions: (q) Pd/C, MeOH, rt, 3 h, quant; (r) *n*-BuLi, B(Oi-Pr)₃, THF, −78 °C to rt, 16 h, 57%; (s) Pd/C, MeOH, rt, 3 h, quant; (t) Pd₂(dba)₃, X-Phos, K₂CO₃, THF, H₂O, 95 °C; (u) TBAF, THF, 0 °C then rt, 16 h.

Based on the above results, we could make the following conclusions regarding the SAR study: (i) the carbonyl group at the C-9 position greatly enhances the E_{max} value; (ii) the presence of a hydroxy group at the C-4 position contributes to

a reduction in the EC₅₀ value; (iii) the presence of a single bond between C-7 and C-8 is more advantageous for activation than a double bond; (iv) the absence of a hydroxy group at the C-2' position contributes to a reduction in the EC₅₀ value; and (v) reduction of the double bond between C-8' and C-9' may likely improve the activity.

In addition, we synthesized compounds 15–17 to probe the necessity for the presence of alkoxy groups and gain insight into their ideal length. As no significant differences were observed between 13 and 15–17 (Supplementary Figure 1), it was apparent that the intensity of the agonistic activity was independent of the presence or length of the *n*-alkoxy group.

Binding Mode Analysis of 13. To explore the molecular basis of the interaction between RXR α and the prepared synthetic ligands, we carried out receptor–ligand docking simulations using the Autodock Vina program,³³ and the best-calculated affinities of the prepared compounds are displayed in Table 1. Because docked binding poses of 1–14 were similar to the crystal structure of the honokiol derivative reported by Scheepstra et al., the results of our docking simulations were likely to be real (Supplementary Figure 2). Thus, compound 13 displayed the most potent activity among the molecules evaluated in this study, and Figure 2 shows the docking pose and the predicted interactions between RXR α LBD and 13. Previous studies indicated that RXR α agonists interacted with Arg316 and Ala327 via a carboxyl group by forming hydrogen bonds, which contributed to an affinity for the receptor.^{28–30} As expected, our docking studies showed that the ester moiety of 13 forms three hydrogen bonds with Arg316 and one hydrogen bond with Ala327. Although no meaningful findings about the advantages of the single bond between C-7 and C-8 were obtained from the results of our docking studies, it was considered that it could affect the orientation of the proton acceptors. Additionally, the docking studies suggested hydrogen bond formation between the hydroxy group at C-4 and the Asn306 residue, which contributes to improved binding to the receptor, and results in an enhanced potency. Furthermore, the aromatic ring within fragment A was predicted to form a π – π T-shaped interaction with the Phe313 residue. Our results also revealed that almost all amino acid residues interacting with fragment A are localized in H5 and in the β -turn between H5 and H6 (Figure 2b). Compared with the crystal structures of liganded RXR α and those of apo-RXR α ,^{3,34,35} only minor alterations in the structures surrounding H5 and the β -turn were displayed before and after ligand binding (Figure 2c). These findings indicate that the structure of fragment A in the evaluated molecules plays an important role in the binding of the molecule to the receptor, and 3-substituted 4-hydroxy-7,8-dihydrocinnamic acid is the optimal substitution of fragment A for efficient binding to H5 and the β -turn.

In contrast, the moiety derived from fragment B occupied the hydrophobic part within the ligand-binding pocket of holo-RXR α and appeared to interact with Ile268, Ile324, Ile345, Phe346, Val349, and Cys432 through electrostatic interactions (Figures 2a and 2d). From the crystallographic analysis, these residues were determined to be localized in the H3 (Ile268), β -turn (Ile324), H7 (Ile345, Phe346, and Val349), and H11 (Cys432) segments of the receptor. Among the helices, the structures of H3 and H11 were drastically altered upon ligand binding, as evaluated by structural studies of RXR α .^{3,4} When the ligand is attracted to the ligand binding pocket of apo-RXR α , H-11 is pushed by the ligand and is repositioned to

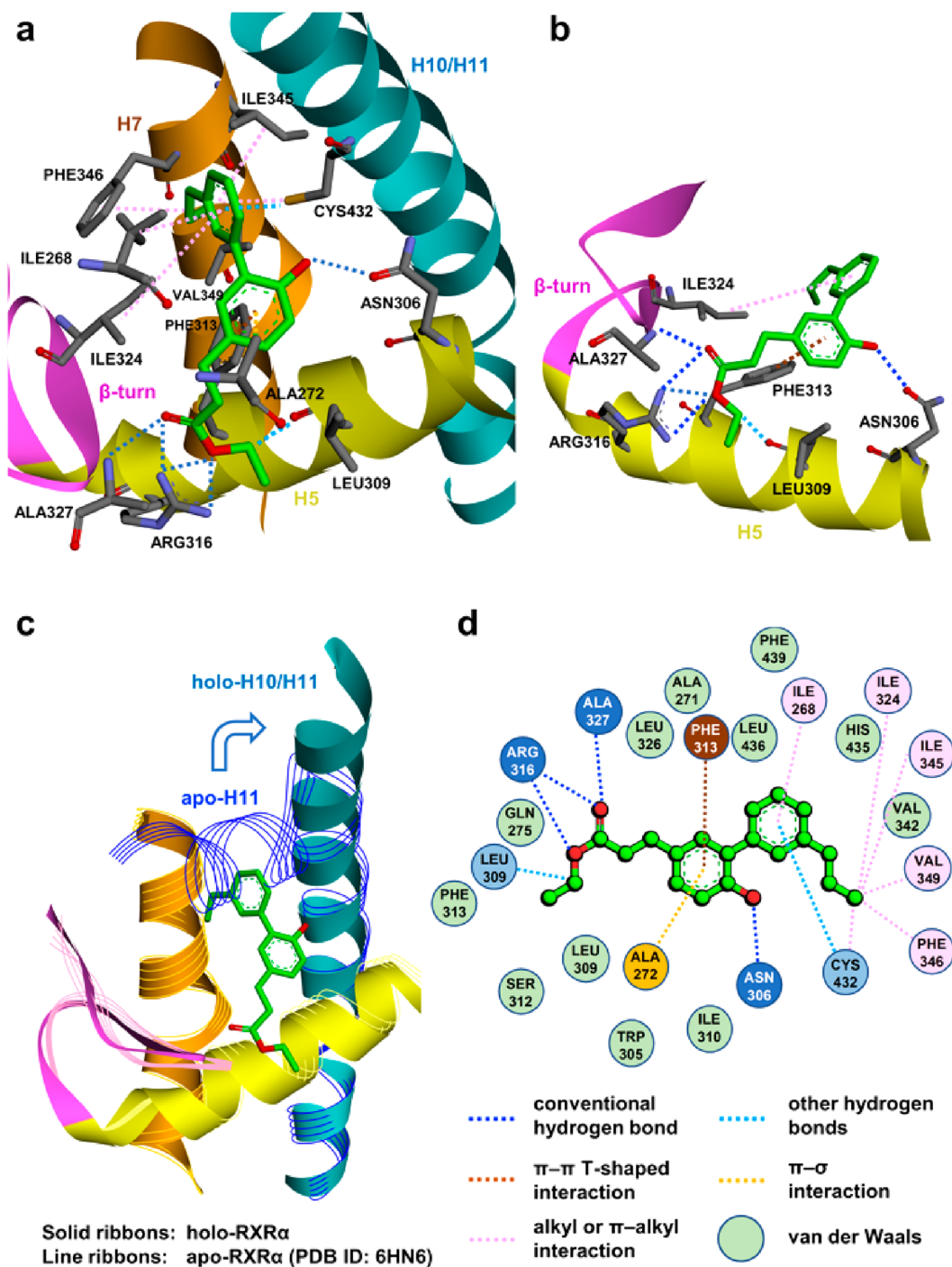


Figure 2. Docked models of 13 with RXR α LBD (PDB ID: 5MKU). Dashed lines indicate nonbonded interactions, including conventional hydrogen bonds (blue), other hydrogen bonds (π -donor or carbon hydrogen bonds; aqua), π - π T-shaped interactions (brown), π - σ interactions (orange), and alkyl or π -alkyl interactions (magenta). (a) All interactions are between 13 and RXR α LBD. The amino acid residues displaying interactions with 13 are depicted. (b) Detected interactions between 13 and H5/ β -turn. (c) Docked models superimposed with the ribbon diagram of apo-RXR α LBD (the structure is PDB entry 6HN6 [3]). The ribbon diagrams of the docked model and apo-RXR α LBD are depicted with solid ribbons and line ribbons, respectively. (d) 2D diagram showing all interactions between 13 and RXR α LBD.

form a continuous helix with H10. Meanwhile, H12 is also repositioned by its hydrophobic interactions with H3 and H4. Furthermore, the transient conformational changes of the C-terminal H11 and H12 were accompanied by the bending of H3 toward the ligands. Consequently, H3–5 and H12 form the AF-2 surface, which is a coregulator binding site in holo-RXR α . As the moiety derived from fragment B was positioned near the position where H11 was originally located in its apo

form (Figure 2c),³ the structure derived from fragment B would be expected to mainly play a role in pushing H11 and inducing the conformational transient. From the results of our docking studies, it is difficult to deduce the reason for the observed enhancement in potency due to the absence of a hydroxy group at the C-2' position. However, the absence of this hydroxy group and the presence of a hydroxy group at the C-4 position were effective for enhancing the affinities with

LBD, considering the outstanding EC_{50} values (23.0 and 12.7 μ M, respectively) and calculated affinities (-11.1 and -11.2 kcal/mol, respectively) observed for **9** and **13** (Table 1). As mentioned above, the hydroxy group at C-4 presumably assists ligand binding to H5, which suggests that the moiety derived from fragment A with a hydroxy group at the C-4 position binds to the receptor in a more precise manner. In this precise conformation, the hydroxy group at C-2' appears to hinder the increased affinity of molecular binding with RXR α .

Moreover, LC-MS analyses revealed that the ester bond of **13** was gradually hydrolyzed in the culture supernatant of the HEK293 cells (Supplementary Figure 3). Since **15** may possibly activate RXR α as an active metabolite, receptor–ligand docking simulations between **15** and RXR α LBD were also performed. As a result, no significant difference in affinity (-11.2 kcal/mol) or docking pose (Supplementary Figure 4) were observed between the two compounds. In addition, considering the finding that **15** activated RXR α to the same extent as **13**, some or all of the RXR α agonistic effects of **13** seemed to be activation of the receptor by **15**.

Activating Efficiency of 13 for the PPAR Subtypes. We next investigated the variation in the activating efficiency of **13** for each PPAR subtype, as the subtle but significant PPAR γ agonistic effect of honokiol has been previously reported.^{36,37} The full lengths of the PPAR α , PPAR γ , and PPAR δ expression vectors were used for the study of the luciferase reporter gene assay. Luciferase reporter assays for PPAR γ and PPAR δ were performed using HEK293 cells, as well as for RXR α , while the assay for PPAR α was performed using HepG2 cells because the high background PPAR α activity in HEK293 cells masked the activities of the test samples. Surprisingly, **13** appeared to exhibit selective activation of PPAR δ (E_{max} 193%, EC_{50} 0.92 μ M; Figure 3a) with a stronger efficacy compared to those of PPAR α (E_{max} 22%, EC_{50} 0.55 μ M; Figure 3b) and PPAR γ (E_{max} 14%, EC_{50} 0.23 μ M; Figure 3c). Furthermore, the E_{max} for PPAR δ of **13** was 193%, indicating that **13** displayed significantly stronger activation than that of even GW501516, an existing PPAR δ -selective agonist. The PPAR δ agonistic activity was sustained with the significant up-regulation of the adipose differentiation-related protein (*Adfp*) mRNA, a PPAR δ -specific target gene³⁸ obtained from the liver of mice treated with a single shot of **13** (100 mg/kg body weight; Figure 3d).

In general, PPAR δ forms permissive heterodimers with RXR in the activated conformation, where PPAR δ presumably dimerizes with endogenous RXR in cells. The effects on the PPAR δ -RXR heterodimer were measured in the reporter gene assay using full-length expression vectors, thereby allowing us to assume that **13** activates the PPAR δ -RXR heterodimer through the activation of RXR. To explore the involvement of the RXR agonistic activity of **13** on the PPAR δ activity in the assay using full-length expression vectors, we examined the effect of PA452, an RXR pan-antagonist,³⁹ on the activity of **13**. We confirmed in advance that the RXR α agonistic activity of **13** was completely inhibited by PA452 in a manner similar to that seen with bexarotene (Figure 4a). The effect of PA452 against the PPAR δ -RXR agonistic activity of **13** was then evaluated by the luciferase reporter gene assay using PPAR δ expression vectors. The obtained results indicated that the PPAR δ -RXR activity of **13** was significantly inhibited by PA452, whereas the activity of GW501516 was not affected (Figure 4b). It was therefore assumed that PA452 interfered with the binding of the RXR agonist to RXRs, and inhibited

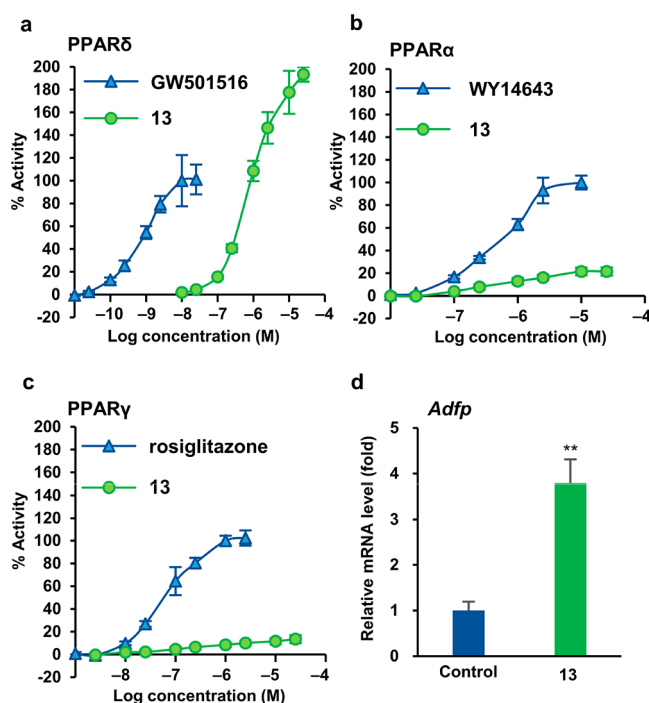


Figure 3. Effects of **13** on RXR heterodimers with each PPAR subtypes. (a–c) Effects of **13** on PPAR δ (a), PPAR α (b), and PPAR γ (c) in the luciferase reporter assay using PPRE-Luc plasmids. Data presented are means \pm SD of three biological replicates. (d) Effect of **13** on the expression of *adfp* mRNA in the liver. Data are represented as mean \pm SE (SE is standard error; one-way ANOVA with Tukey Kramer test, ** indicates $p < 0.01$ versus the control).

the transcriptional activation of RXR α homodimers by RXR agonists. While PA452 was unable to inhibit the transcriptional activation of PPAR δ -RXR heterodimers by a conventional PPAR δ agonist that binds to PPAR δ (e.g., GW501516), it successfully inhibited the transcriptional activation of PPAR δ -RXR heterodimers by **13**. These observations indicated a reasonable possibility that PA452 blocked the PPAR δ agonistic activity of **13** by interfering with the binding between RXR LBD and **13** (Figure 4c), thereby indicating that the PPAR δ -RXR agonistic activity of **13** is induced to an extent via binding to RXR LBD. Furthermore, it was presumed that PPAR δ LBD is also involved in the activation of the PPAR δ -RXR heterodimer by **13**, because GSK0660, which is a PPAR δ antagonist, also inhibited the PPAR δ -RXR agonistic activity of **13** (Figure 4b). To evaluate the “true” PPAR δ agonistic activity of **13**, we performed reporter gene assays using the Gal4 hybrid system. Because the cells in these assays express a hybridized receptor in which the N-terminal DNA binding domain (DBD) of PPAR δ has been replaced by Gal4 DBD, when the ligand binds to PPAR δ LBD, Gal4 DBD binds to the upstream activation sequence (UAS) on the reporter gene.⁴⁰ As a result, the “true” PPAR δ agonistic activities excluding the effect of the heterodimer can be measured. More specifically, compound **13** exhibited little activation of PPAR δ (E_{max} 6.3%) in the assay using the Gal4 hybrid system (Figure 4d). Although the PPAR δ agonistic activity of **13** was weak, it was detected with statistical significance, unlike in the case of **14**, which showed no activation for the PPAR δ -RXR heterodimer (Supplementary Figures 5 and 6). Overall, the finding that **13** activates PPAR δ -RXR heterodimers significantly more potently than the monomeric PPAR δ suggests that the particularly weak

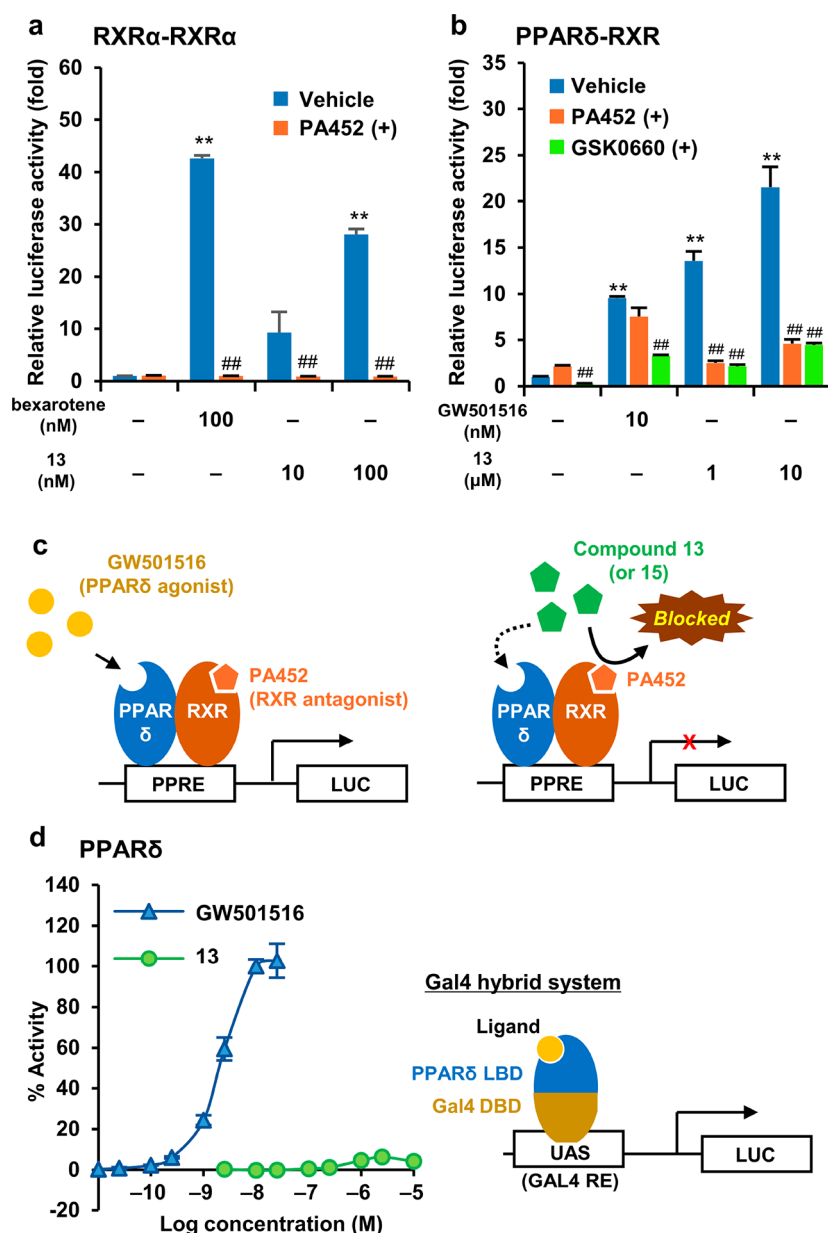


Figure 4. PPAR δ -RXR agonistic activity of 13 is probably mainly due to the activation of RXR. (a, b) Effects of antagonists on the RXR α agonistic activity (a) and the PPAR δ agonistic activity (b) of 13 in the luciferase reporter assay. Data presented are means \pm SD of three biological replicates (two-way ANOVA with Tukey Kramer test, ** indicates $p < 0.01$ versus the control, ### indicates $p < 0.01$ versus the groups without antagonist treatment). (c) Plausible mechanism of PPAR δ -RXR activation by 13. GW501516 activated the PPAR δ -RXR heterodimer even in the presence of PA452 (left), whereas 13 was unable to activate the heterodimer in the presence of PA452 (right). (d) Effects of 13 on PPAR δ in the reporter gene assay using the Gal4 hybrid receptor. GW501516 was used as the positive control. Data are represented as mean \pm SD of three biological replicates.

PPAR δ agonistic activity of 13 is synergistically enhanced by its own RXR agonistic activity. As a result of evaluating the activities of compounds 1–14 toward the PPAR δ -RXR heterodimer, compounds 7, 9, and 11, for which the EC_{50} values were 3.30, 1.34, and 6.12 μ M, respectively, were also found to exhibit strong activities at a concentration of 10 μ M (Supplementary Figure 5). Therefore, the presence of a single bond between C-7 and C-8, and the presence of a hydroxy group at the C-4 position were considered crucial to give a strong activity toward the PPAR δ -RXR heterodimer.

CONCLUSION

We herein reported the synthesis of magnaldehyde B along with its more potent analogs for screening of their RXR α

agonistic activities. Although several PPAR δ -selective agonists that bind to PPAR δ LBD have been developed, to the best of our knowledge, PPAR δ /RXR dual-agonists had yet to be reported. We note that activation of the PPAR δ -RXR heterodimer by a nonconventional mechanism has the potential to solve the issues that have previously hindered the development of drugs targeting PPAR δ . Thus, our molecular design and SAR studies revealed that the maximum PPAR δ activity was achieved for structure 13, and this activity was double that revealed by the luciferase reporter gene assay for the reported agonist GW501516, thereby suggesting that RXR-targeted agonists may activate the receptor more efficiently than conventional PPAR δ -targeted agonists. However, comparison of EC_{50} values showed that the PPAR δ -RXR

agonistic activity of **13** was not as potent as that of GW501516, suggesting the need to further refine the structure to improve its potency. It should be noted that evaluation of the action of the prepared compounds for activation to other RXR-NR heterodimers has yet to be conducted, and so the possibility for side effects cannot be ruled out at this time. However, the new molecular class of agonists developed in this study show great potential for improving human health, as the use of strategies for targeting PPAR δ has broader implications due to the fact that this receptor is believed to be a therapeutic target for metabolic disorders, including obesity, type 2 diabetes mellitus, dyslipidaemia, and nonalcoholic fatty liver disease. In ongoing research, we aim to further refine the structure, taking into account the bioavailability and evaluating its effect in animal models for diseases.

METHODS

Detailed methods are provided in the [Supporting Information](#).

ASSOCIATED CONTENT

Supporting Information

The Supporting Information is available free of charge at <https://pubs.acs.org/doi/10.1021/acschembio.0c00146>.

Detailed methods, materials, supplementary figures, and characterization data including ^1H and ^{13}C NMR spectra of all compounds (PDF)

Docked files of compounds **13** and **15**(ZIP)

AUTHOR INFORMATION

Corresponding Author

Ken-ichi Nakashima – Laboratory of Medicinal Resources, School of Pharmacy, Aichi Gakuin University, Nagoya 464-8650, Japan; orcid.org/0000-0002-3050-9903; Email: nakasima@dpc.agu.ac.jp

Authors

Eiji Yamaguchi – Laboratory of Pharmaceutical Synthetic Chemistry, Gifu Pharmaceutical University, Gifu 501-1196, Japan; orcid.org/0000-0002-1167-8832

Chihaya Noritake – Laboratory of Medicinal Resources, School of Pharmacy, Aichi Gakuin University, Nagoya 464-8650, Japan

Yukari Mitsugi – Laboratory of Pharmaceutical Synthetic Chemistry, Gifu Pharmaceutical University, Gifu 501-1196, Japan

Mayuki Goto – Laboratory of Pharmaceutical Synthetic Chemistry, Gifu Pharmaceutical University, Gifu 501-1196, Japan

Takao Hirai – Laboratory of Medicinal Resources, School of Pharmacy, Aichi Gakuin University, Nagoya 464-8650, Japan

Naohito Abe – Laboratory of Pharmacognosy, Gifu Pharmaceutical University, Gifu 501-1196, Japan

Eiji Sakai – Laboratory of Herbal Garden, Gifu Pharmaceutical University, Gifu 501-1196, Japan

Masayoshi Oyama – Laboratory of Pharmacognosy, Gifu Pharmaceutical University, Gifu 501-1196, Japan

Akichika Itoh – Laboratory of Pharmaceutical Synthetic Chemistry, Gifu Pharmaceutical University, Gifu 501-1196, Japan; orcid.org/0000-0003-3769-7406

Makoto Inoue – Laboratory of Medicinal Resources, School of Pharmacy, Aichi Gakuin University, Nagoya 464-8650, Japan

Complete contact information is available at:

<https://pubs.acs.org/10.1021/acschembio.0c00146>

Author Contributions

[†]K.N. and E.Y. contributed equally to this work.

Notes

The authors declare no competing financial interest.

ACKNOWLEDGMENTS

This study was supported by JSPS KAKENHI Grant 17K08352. The authors thank M. Makishima at Nihon University, School of Medicine for providing the RXR expression vector and the reporter plasmid. We also thank K. Inoue at Gifu Pharmaceutical University for assistance with the isolation of magnaldehyde B. We would like to thank Editage (www.editage.jp) for English language editing.

REFERENCES

- (1) Nuclear Receptors Nomenclature Committee. (1999) A Unified Nomenclature System for the Nuclear Receptor Superfamily. *Cell* 97, 161–163.
- (2) Germain, P., Staels, B., Dacquet, C., Spedding, M., and Laudet, V. (2006) Overview of Nomenclature of Nuclear Receptors. *Pharmacol. Rev.* 58, 685–704.
- (3) Eberhardt, J., McEwen, A. G., Bourguet, W., Moras, D., and Dejaegere, A. (2019) A Revisited Version of the Apo Structure of the Ligand-Binding Domain of the Human Nuclear Receptor Retinoic X Receptor α . *Acta Crystallogr., Sect. F: Struct. Biol. Commun.* 75, 98–104.
- (4) Wurtz, J. M., Bourguet, W., Renaud, J. P., Vivat, V., Chambon, P., Moras, D., and Gronemeyer, H. (1996) A Canonical Structure for the Ligand-Binding Domain of Nuclear Receptors. *Nat. Struct. Biol.* 3, 87–94.
- (5) Renaud, J. P., Rochel, N., Ruff, M., Vivat, V., Chambon, P., Gronemeyer, H., and Moras, D. (1995) Crystal Structure of the RAR- γ Ligand-Binding Domain Bound to *all-trans* Retinoic Acid. *Nature* 378, 681–689.
- (6) Kojetin, D. J., Matta-Camacho, E., Hughes, T. S., Srinivasan, S., Nwachukwu, J. C., Cavett, V., Nowak, J., Chalmers, M. J., Marciano, D. P., Kamenecka, T. M., Shulman, A. I., Rance, M., Griffin, P. R., Bruning, J. B., and Nettles, K. W. (2015) Structural Mechanism for Signal Transduction in RXR Nuclear Receptor Heterodimers. *Nat. Commun.* 6, 8013.
- (7) Westin, S., Kurokawa, R., Nolte, R. T., Wisely, G. B., McInerney, E. M., Rose, D. W., Milburn, M. V., Rosenfeld, M. G., and Glass, C. K. (1998) Interactions Controlling the Assembly of Nuclear-Receptor Heterodimers and Co-Activators. *Nature* 395, 199–202.
- (8) Shulman, A. I., Larson, C., Mangelsdorf, D. J., and Ranganathan, R. (2004) Structural Determinants of Allosteric Ligand Activation in RXR Heterodimers. *Cell* 116, 417–429.
- (9) Lefebvre, P., Benomar, Y., and Staels, B. (2010) Retinoid X Receptors: Common Heterodimerization Partners with Distinct Functions. *Trends Endocrinol. Metab.* 21, 676–683.
- (10) DiRenzo, J., Soderstrom, M., Kurokawa, R., Ogliastro, M. H., Ricote, M., Ingrey, S., Horlein, A., Rosenfeld, M. G., and Glass, C. K. (1997) Peroxisome Proliferator-Activated Receptors and Retinoic Acid Receptors Differentially Control the Interactions of Retinoid X Receptor Heterodimers with Ligands, Coactivators, and Corepressors. *Mol. Cell. Biol.* 17, 2166–2176.
- (11) Mirza, A. Z., Althagafi, I. I., and Shamshad, H. (2019) Role of PPAR Receptor in Different Diseases and Their Ligands: Physiological Importance and Clinical Implications. *Eur. J. Med. Chem.* 166, 502–513.
- (12) Gross, B., Pawlak, M., Lefebvre, P., and Staels, B. (2017) PPARs in Obesity-Induced T2DM, Dyslipidaemia and NAFLD. *Nat. Rev. Endocrinol.* 13, 36–49.
- (13) Kubota, N., Terauchi, Y., Miki, H., Tamemoto, H., Yamauchi, T., Komeda, K., Satoh, S., Nakano, R., Ishii, C., Sugiyama, T., Eto, K.,

- Tsubamoto, Y., Okuno, A., Murakami, K., Sekihara, H., Hasegawa, G., Naito, M., Toyoshima, Y., Tanaka, S., Shiota, K., Kitamura, T., Fujita, T., Ezaki, O., Aizawa, S., Nagai, R., Tobe, K., Kimura, S., and Kadowaki, T. (1999) PPAR Gamma Mediates High-Fat Diet-Induced Adipocyte Hypertrophy and Insulin Resistance. *Mol. Cell* 4, 597–609.
- (14) Nanjan, M. J., Mohammed, M., Prashantha Kumar, B. R., and Chandrasekar, M. J. N. (2018) Thiazolidinediones as Antidiabetic Agents: A Critical Review. *Bioorg. Chem.* 77, 548–567.
- (15) Chigurupati, S., Dhanaraj, S. A., and Balakumar, P. (2015) A Step Ahead of PPAR γ Full Agonists to PPAR γ Partial Agonists: Therapeutic Perspectives in the Management of Diabetic Insulin Resistance. *Eur. J. Pharmacol.* 755, 50–57.
- (16) Weihrauch, M., and Handschin, C. (2018) Pharmacological Targeting of Exercise Adaptations in Skeletal Muscle: Benefits and Pitfalls. *Biochem. Pharmacol.* 147, 211–220.
- (17) Sahebkar, A., Chew, G. T., and Watts, G. F. (2014) New Peroxisome Proliferator-Activated Receptor Agonists: Potential Treatments for Atherogenic Dyslipidemia and Non-Alcoholic Fatty Liver Disease. *Expert Opin. Pharmacother.* 15, 493–503.
- (18) Vazquez-Carrera, M. (2016) Unraveling the Effects of PPAR β/δ on Insulin Resistance and Cardiovascular Disease. *Trends Endocrinol. Metab.* 27, 319–334.
- (19) Palomer, X., Barroso, E., Pizarro-Delgado, J., Pena, L., Botteri, G., Zarei, M., Aguilar, D., Montori-Grau, M., and Vazquez-Carrera, M. (2018) PPAR β/δ : A Key Therapeutic Target in Metabolic Disorders. *Int. J. Mol. Sci.* 19, 913.
- (20) Fan, W., Waizenegger, W., Lin, C. S., Sorrentino, V., He, M. X., Wall, C. E., Li, H., Liddle, C., Yu, R. T., Atkins, A. R., Auwerx, J., Downes, M., and Evans, R. M. (2017) PPAR δ Promotes Running Endurance by Preserving Glucose. *Cell Metab.* 25, 1186–11933.
- (21) Li, D., Li, T., Wang, F., Tian, H., and Samuels, H. H. (2002) Functional Evidence for Retinoid X Receptor (RXR) as a Nonsilent Partner in the Thyroid Hormone Receptor/RXR Heterodimer. *Mol. Cell. Biol.* 22, 5782–5792.
- (22) de Lera, A. R., Bourguet, W., Altucci, L., and Gronemeyer, H. (2007) Design of Selective Nuclear Receptor Modulators: RAR and RXR as a Case Study. *Nat. Rev. Drug Discovery* 6, 811–820.
- (23) Leibowitz, M. D., Ardecky, R. J., Boehm, M. F., Broderick, C. L., Carfagna, M. A., Crombie, D. L., D'Arrigo, J., Etgen, G. J., Faul, M. M., Grese, T. A., Havel, H., Hein, N. I., Heyman, R. A., Jolley, D., Klausung, K., Liu, S., Mais, D. E., Mapes, C. M., Marschke, K. B., Michellys, P. Y., Montrose-Rafizadeh, C., Ogilvie, K. M., Pascual, B., Rungta, D., Tyhonas, J. S., Urcan, M. S., Wardlow, M., Yumibe, N., and Reifel-Miller, A. (2006) Biological Characterization of a Heterodimer-Selective Retinoid X Receptor Modulator: Potential Benefits for the Treatment of Type 2 Diabetes. *Endocrinology* 147, 1044–1053.
- (24) Morishita, K., and Kakuta, H. (2017) Retinoid X Receptor Ligands with Anti-Type 2 Diabetic Activity. *Curr. Top. Med. Chem.* 17, 696–707.
- (25) Cramer, P. E., Cirrito, J. R., Wesson, D. W., Lee, C. Y., Karlo, J. C., Zinn, A. E., Casali, B. T., Restivo, J. L., Goebel, W. D., James, M. J., Brunden, K. R., Wilson, D. A., and Landreth, G. E. (2012) ApoE-Directed Therapeutics Rapidly Clear β -Amyloid and Reverse Deficits in AD Mouse Models. *Science* 335, 1503–1506.
- (26) Kotani, H., Tanabe, H., Mizukami, H., Makishima, M., and Inoue, M. (2010) Identification of a Naturally Occurring Retinoid, Honokiol, that Activates the Retinoid X Receptor. *J. Nat. Prod.* 73, 1332–1336.
- (27) Yahara, S., Nishiyori, T., Kohda, A., Nohara, T., and Nishioka, I. (1991) Isolation and Characterization of Phenolic Compounds from Magnoliae Cortex Produced in China. *Chem. Pharm. Bull.* 39, 2024–2036.
- (28) Nakashima, K., Murakami, T., Tanabe, H., and Inoue, M. (2014) Identification of a Naturally Occurring Retinoid X Receptor Agonist from Brazilian Green Propolis. *Biochim. Biophys. Acta, Gen. Subj.* 1840, 3034–3041.
- (29) Hiromori, Y., Aoki, A., Nishikawa, J., Nagase, H., and Nakanishi, T. (2015) Transactivation of the Human Retinoid X Receptor by Organotins: Use of Site-Directed Mutagenesis to Identify Critical Amino Acid Residues for Organotin-Induced Transactivation. *Metallomics* 7, 1180–1188.
- (30) Wang, G. H., Jiang, F. Q., Duan, Y. H., Zeng, Z. P., Chen, F., Dai, Y., Chen, J. B., Liu, J. X., Liu, J., Zhou, H., Chen, H. F., Zeng, J. Z., Su, Y., Yao, X. S., and Zhang, X. K. (2013) Targeting Truncated Retinoid X Receptor-A by CF31 Induces TNF- α -Dependent Apoptosis. *Cancer Res.* 73, 307–318.
- (31) Scheepstra, M., Nieto, L., Hirsch, A. K. H., Fuchs, S., Leysen, S., Lam, C. V., in het Panhuis, L., van Boeckel, C. A. A., Wienk, H., Boelens, R., Ottmann, C., Milroy, L.-G., and Brunsveld, L. (2014) A Natural-Product Switch for a Dynamic Protein Interface. *Angew. Chem., Int. Ed.* 53, 6443–6448.
- (32) Scheepstra, M., Andrei, S. A., de Vries, R. M. J. M., Meijer, F. A., Ma, J. N., Burstein, E. S., Olsson, R., Ottmann, C., Milroy, L. G., and Brunsveld, L. (2017) Ligand Dependent Switch from RXR Homo- to RXR-NURR1 Heterodimerization. *ACS Chem. Neurosci.* 8, 2065–2077.
- (33) Trott, O., and Olson, A. J. (2009) AutoDock Vina: Improving the Speed and Accuracy of Docking with a New Scoring Function, Efficient Optimization and Multithreading. *J. Comput. Chem.* 31, 455–461.
- (34) Bourguet, W., Vivat, V., Wurtz, J. M., Chambon, P., Gronemeyer, H., and Moras, D. (2000) Crystal Structure of a Heterodimeric Complex of RAR and RXR Ligand-Binding Domains. *Mol. Cell* 5, 289–298.
- (35) Egea, P. F., Mitschler, A., and Moras, D. (2002) Molecular Recognition of Agonist Ligands by RXRs. *Mol. Endocrinol.* 16, 987–997.
- (36) Atanasov, A. G., Wang, J. N., Gu, S. P., Bu, J., Kramer, M. P., Baumgartner, L., Fakhrudin, N., Ladurner, A., Malainer, C., Vuorinen, A., Noha, S. M., Schwaiger, S., Rollinger, J. M., Schuster, D., Stuppner, H., Dirsch, V. M., and Heiss, E. H. (2013) Honokiol: A Non-Adipogenic Ppar γ Agonist from Nature. *Biochim. Biophys. Acta, Gen. Subj.* 1830, 4813–4819.
- (37) Dreier, D., Resetar, M., Temml, V., Ryczek, L., Kratena, N., Schnurch, M., Schuster, D., Dirsch, V. M., and Mihovilovic, M. D. (2018) Magnolol Dimer-Derived Fragments as Ppar γ -Selective Probes. *Org. Biomol. Chem.* 16, 7019–7028.
- (38) Bojic, L. A., Telford, D. E., Fullerton, M. D., Ford, R. J., Sutherland, B. G., Edwards, J. Y., Sawyez, C. G., Gros, R., Kemp, B. E., Steinberg, G. R., and Huff, M. W. (2014) PPAR δ Activation Attenuates Hepatic Steatosis in Ldlr $^{-/-}$ Mice by Enhanced Fat Oxidation, Reduced Lipogenesis, and Improved Insulin Sensitivity. *J. Lipid Res.* 55, 1254–1266.
- (39) Takahashi, B., Ohta, K., Kawachi, E., Fukasawa, H., Hashimoto, Y., and Kagechika, H. (2002) Novel Retinoid X Receptor Antagonists: Specific Inhibition of Retinoid Synergism in RXR-RAR Heterodimer Actions. *J. Med. Chem.* 45, 3327–3330.
- (40) Bisgaier, C. L., Oniciu, D. C., and Srivastava, R. A. K. (2018) Comparative Evaluation of Gemcabene and Peroxisome Proliferator-Activated Receptor Ligands in Transcriptional Assays of Peroxisome Proliferator-Activated Receptors: Implication for the Treatment of Hyperlipidemia and Cardiovascular Disease. *J. Cardiovasc. Pharmacol.* 72, 3–10.